

Cite this: *Analyst*, 2012, **137**, 4647

www.rsc.org/analyst

COMMUNICATION

Calixarene capped ZnS quantum dots as an optical nanoprobe for detection and determination of menadione†

Kuldeep V. Joshi, Bhoomika K. Joshi, Alok Pandya, Pinkesh G. Sutariya and Shobhana K. Menon*

Received 7th June 2012, Accepted 25th July 2012

DOI: 10.1039/c2an35766f

In this communication we report a *p*-sulfonatocalix[4]arene coated ZnS quantum dots “cup type” highly stable optical probe for the detection and determination of menadione (VK₃) with high sensitivity and selectivity. The detection of VK₃ depends on supramolecular host–guest chemistry.

Vitamin K₃ (VK₃) is a synthetic fat soluble vitamin and is used for blood coagulation and in the bone mineralization process.¹ In recent years, it has drawn huge attention due to its remarkable anticancer properties.² VK₃ contains a naphthoquinone ring, and its basic structure is 2-methyl-1,4-naphthoquinone. These vitamins are named according to their side chains by forming new derivatives. VK₃ is obtained synthetically without a side chain and is named menadione. The physiological activity of VK₃ is the strongest among the K group vitamins. It shows antitumor and anti-inflammatory activity because of the quinone group in its structure. In a series of *in vitro* and *in vivo* animal studies, VK₃ showed significant antineoplastic activities against both malignant cell lines and a variety of human tumor cells.²

There are several methods reported for the detection and determination of VK₃ such as spectrophotometric, electrochemical, colorimetric reaction, *etc.*³ which are frequently used although these approaches are time consuming, laborious, expensive and less sensitive. It is crucial to develop sensitive and rapid analytical methods for the estimation of VK₃ due to its wide use in chemical, biological and pharmaceutical areas. Herein we report for the first time the trace level detection of VK₃ using a nanosensor.

Supramolecular based nanosensors are an upcoming research area for recognition of biomolecules, organic molecules and metals. Crown and β -cyclodextrin coated nanoparticles (NPs) have already been reported as optical sensors for metal and polycyclic aromatic hydrocarbons (PAHs).⁴ Calixarenes are the third generation of host molecules and effective sensing probes for the detection of ions and neutral molecules due to their low toxicity and have excellent complexation ability.⁵ Our research group has reported earlier sensitive sensors for ions such as K⁺ and sulphide as well as biomolecules like amino acids.⁶ Recently, many calixarenes coated semiconductor NPs were reported as fluorescent sensors of metals,

pesticides, amino acids, organic molecules and neurotransmitters.⁷ Calixarene-quantum dot systems have been developed as stable fluorescent chemosensors for biomolecules recognition.

Quantum dots (QDs) have an exclusive size dependent optical property. This property has made them a powerful molecular recognition tool compared to the traditional organic dyes. There are many biological and metal sensors developed based on fluorescence changes of QDs, induced by chemical modification.⁸ ZnSQDs have a wide band gap at room temperature, high index of refraction and high transmittance in the visible range.⁹ Due to these properties ZnSQDs have been used widely as an important phosphor for photoluminescence, electroluminescence and cathodoluminescence. ZnSQDs can be synthesized in an aqueous medium, and they are less expensive and least toxic than any other semiconductor QDs with good photocatalytic properties and hence were found suitable for biological and medical applications. Recently, some reports have been published in which ZnSQDs are used as chemical and biosensors.¹⁰

In this communication we synthesized ZnSQDs by a soft chemical method as reported by M. Chatterjee *et al.*¹¹ with some modifications (ESI†). The resulting ZnSQDs were capped with poly vinyl-pyrrolidone (PVP) molecules by a co-ordinate bond between the nitrogen of PVP and Zn²⁺. The optical property of NPs increased and was secured for a long time by the coating of *p*-sulfonatocalix[*n*]arene.¹²

Herein, we used *p*-sulfonatocalix[4]arene (pSC[4]A) as the surface-coating agent for the PVP capped ZnSQDs to enhance and preserve its optical properties. pSC[4]A was prepared according to a method reported earlier.¹³ pSC[4]A coated ZnSQDs were prepared by mixing ZnSQDs with pSC[4]A in tetrahydrofuran at room temperature (ESI†). FT-IR spectra of pure pSC[4]A reveal the characteristic peak of the calix moiety at 1430 cm^{−1} (benzene ring stretching); 2840, 2910 cm^{−1} (CH₂); 690, 810 cm^{−1} (aromatic ring); 3422 cm^{−1} (OH) which are also observed in pSC[4]A–ZnSQDs with minor changes (Fig. S1, ESI†). Comparing both spectra, a significant variation has been observed; the peak intensity of –OH found in pure pSC[4]A reduces in pSC[4]A–ZnSQDs. This result clearly indicates that the –OH group of the lower edge of pSC[4]A interacts with PVP capped ZnSQDs and forms a hydrogen bond (O⋯H⋯O) during the coating process and a “cup like” assembly.¹⁴

Fig. 1(A) shows the fluorescence (FL) spectra of ZnSQDs and *p*-SC[4]A coated ZnSQDs. It reveals that emission properties of ZnSQDs increased with a small shift towards longer wavelength (red shift, 2 nm: 480 → 482 nm) in the presence of pSC[4]A. Under the

Department of Chemistry, School of Sciences, Gujarat University, Ahmedabad, Gujarat-380009, India. E-mail: shobhanamenon07@gmail.com; Fax: +91 79 26308545; Tel: +91 79 26302286

† Electronic supplementary information (ESI) available. See DOI: 10.1039/c2an35766f

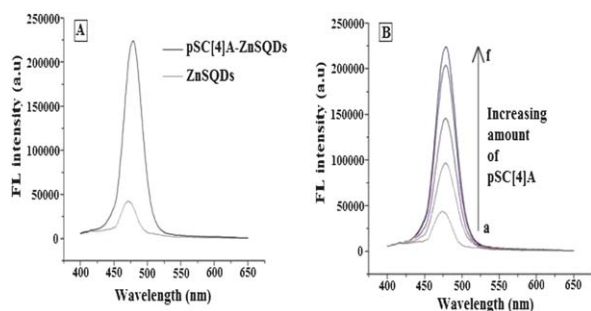


Fig. 1 (A) FL spectra of pSC[4]A coated and uncoated ZnSQDs. (B) Effect of pSC[4]A on the FL intensity of ZnSQDs (from a to f: 0 , 1×10^{-6} , 5×10^{-6} , 8×10^{-6} , 12×10^{-6} , 15×10^{-6} M).

optimum conditions, FL intensity increases up to 80% upon the addition of pSC[4]A.

Here, the line width of the pSC[4]A coated ZnSQDs FL spectrum is relatively narrow (with the full width at half-maximum of 35 nm), indicating that the coated QDs have a narrow size distribution.

Furthermore, Fig. 1(B) shows that the increasing amount of pSC[4]A enhanced the FL intensity of ZnSQDs dramatically. With increasing concentration of pSC[4]A the hanging bonds and surface defects on the QDs are reduced,¹⁵ hence they become more stable, consequently increasing the FL intensity. After the addition of 15×10^{-6} M pSC[4]A solution, the FL intensity was stable, which indicates that the whole of the surface of ZnSQDs was layered by a large amount of calixarene. In particular, surface defects of QDs are saturated, pSC[4]A traps the defects, resulting in a stable FL suspension.¹⁶ Therefore, a 15×10^{-6} M (50 μ L) solution was selected to prepare pSC[4]A-QDs.

Transmission electron microscopy (TEM) has been used to characterize the ZnSQDs and pSC[4]A-ZnSQDs. The TEM images of ZnSQDs and pSC[4]A-ZnSQDs are shown in Fig. 2A and C respectively, which show that the particles are monodispersed and uniform.

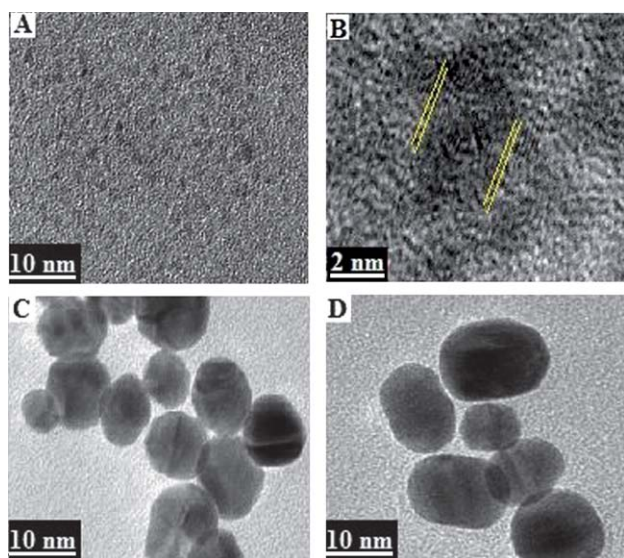


Fig. 2 TEM images of (A) ZnSQDs, (B) HRTEM of ZnSQDs, (C) pSC[4]A-ZnSQDs, (D) after the addition of VK₃ to pSC[4]A-ZnSQDs.

The HRTEM image of ZnSQDs (Fig. 2B) shows the size as ~ 2.0 nm with noticeable lattice fringes, which indicated that the synthesized QDs are crystalline in nature. The diameter of ZnSQDs increases after coating with pSC[4]A. The average sizes of ZnSQDs and pSC[4]A-ZnSQDs are measured by DLS and were found to be 2.0 nm and 30 nm respectively (Fig. S2, ESI[†]). The increase in particle size by DLS measurements and TEM images confirms the surface coating of pSC[4]A on ZnSQDs.

The stability of ZnSQDs and pSC[4]A-ZnSQDs was evaluated in aqueous solution at room temperature (Fig. S3, ESI[†]). It is found that the FL intensity of pSC[4]A-ZnSQDs increased gradually up to 9 days. After that a negligible reduction in FL intensity appeared 3 days later, and then the intensity was stable up to 25 days. In contrast, the intensity of ZnSQDs increases up to 4 days, then suddenly drops, and the FL peak of ZnSQDs is shifted to a longer wavelength, which may be due to the increasing size of QDs or their aggregation with each other. These results of photostability illustrated that pSC[4]A preserves the optical properties of ZnSQDs for a long period of time. The process of preparing pSC[4]A-ZnSQDs reduces the surface defects on QDs, resulting in the formation of more stable pSC[4]A-ZnSQDs.⁸

The effect of pH in the range of 2.0–12.0 was studied in order to select the optimum conditions for the analysis (Fig. S4, ESI[†]). The results obtained from this study show that the FL intensity of pSC[4]A-ZnSQDs was almost stable in the pH range 5.0–10.0. Hence, pH 7.0 was finally selected for further analysis. When the pH is below 5.0, the FL intensity of pSC[4]A-ZnSQDs decreased drastically. It is clear that at lower pH, ZnSQDs dissolve and produce surface defects; thus the FL intensity of pSC[4]A-ZnSQDs also decreases. On the other hand, at a higher pH above 10.0, the electrostatic repulsion between ZnSQDs and the negative charge of the solution prevent agglomeration of NPs, which results in the significant increase of the FL intensity of pSC[4]A-ZnSQDs after pH 10.0.

The responses of different vitamin solutions (50 μ L, 1×10^{-4} M) on the FL intensity of pSC[4]A-ZnSQDs are summarized in Fig. 3. It shows that pSC[4]A-ZnSQDs are sensitive to VK₃ among all other vitamins. The FL intensity was quenched by almost 95% by the VK₃ solution. The remaining vitamins have a slight effect on the FL intensity of pSC[4]A-ZnQDs. It reveals that pSC[4]A-ZnSQDs are highly selective towards VK₃ among the tested vitamins.

The host-guest complexation ability of pSC[4]A and VK₃ has already been investigated¹⁷ showing selectively the binding capacity of pSC[4]A by its hydrophobic cavity. On the basis of this investigation, we expected that the prepared pSC[4]A-ZnSQDs will have a complexing ability towards VK₃ and will facilitate the formulation of a

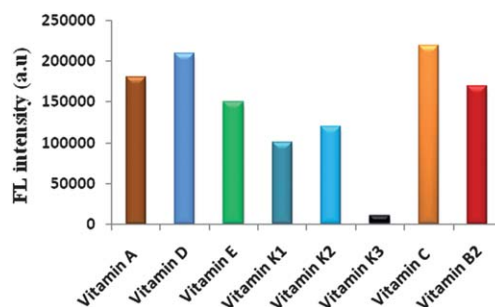


Fig. 3 Effect of relevant vitamins (1×10^{-4} M) on the FL intensity of pSC[4]A-ZnSQDs.

sensitive sensor for VK₃. Fig. 4 shows that the FL intensity of pSC[4]A–ZnSQDs decreases with increasing concentration of VK₃. Quenching started with the addition of 5×10^{-9} M (50 μ L) VK₃. It can be seen that at a higher concentration of VK₃ the maximum shifts toward lower wavelength (blue shift). FL intensity was found to be quenched to the maximum on the addition of 1×10^{-4} M (50 μ L) VK₃.

It is known that a calix can provide accommodation to guest molecules in the cavity, when they are added in solution resulting in an inclusion complex.¹⁸ The reaction between pSC[4]A and ZnSQDs gave rise to a cup type cavity and led to the assembling of an inclusion complex with VK₃ (Fig. 5). The remarkable blue shift (7 nm: 482 \rightarrow 476 nm) in the FL spectra at a higher concentration of VK₃ also gives an indication that VK₃ was located in a more hydrophobic environment, which was supported by the inclusion of VK₃ within the aromatic cavity of pSC[4]A.

Electrostatic, hydrophobic interactions as well as van der Waals interaction, hydrogen bonding and so on cooperatively contribute to the formation of an inclusion complex.

In this context, hydrophobic interaction also contributes to the formation of an inclusion complex. VK₃ is a highly hydrophobic molecule and tries to escape from the polar phase; this property leads to considerable interaction between VK₃ and the nonpolar hydrophobic cavity of pSC[4]A.¹⁹ TEM images (Fig. 2D) also reveal that after the addition of VK₃, no morphological change or aggregation takes place in pSC[4]A–ZnSQDs indicating that there was no chemical reaction taking place on the surface of pSC[4]A between –SO₃H and VK₃.

In order to investigate the main driving force for the interaction between pSC[4]A–ZnSQDs and VK₃, the effect of NaCl ionic strength on the inclusion process was examined. Fig. 6 shows the effect of ionic strength on the fluorescence quenching intensity of pSC[4]A–ZnSQDs and the VK₃ system. As can be seen from the figure, when the NaCl concentration is 0.5 mol L^{–1}, the FL intensity of pSC[4]A–ZnSQDs and VK₃ does not undergo significant change, which demonstrated that the inclusion process was not affected by the ionic strength of NaCl. This means that electrostatic interaction is not the main driving force for the interaction between pSC[4]A–ZnS QDs and VK₃. Therefore, hydrophobic interaction was considered to play the main role in the formation of the host–guest inclusion complex.

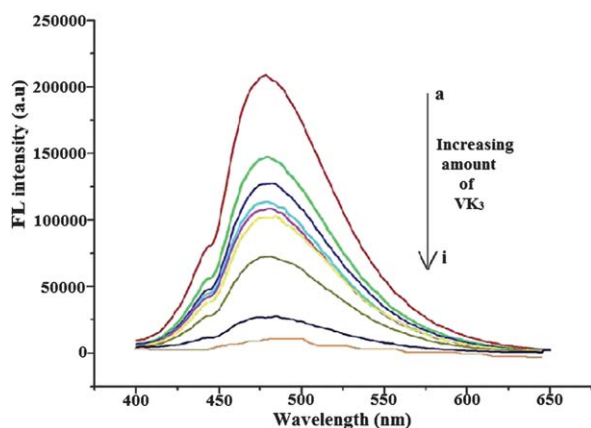


Fig. 4 Effect of VK₃ on the FL intensity of pSC[4]A–ZnSQDs (from a to i: 0, 5×10^{-9} , 1×10^{-8} , 1×10^{-7} , 5×10^{-7} , 9×10^{-7} , 5×10^{-6} , 1×10^{-5} , 1×10^{-4} M).

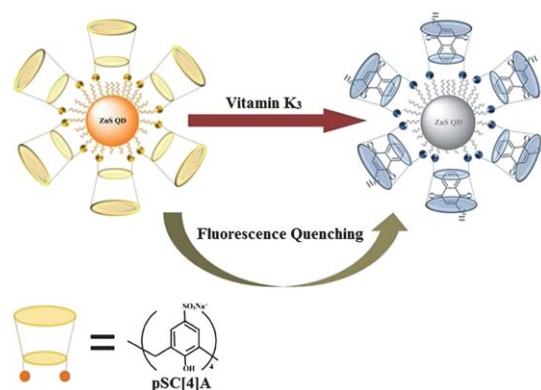


Fig. 5 Schematic representation of a VK₃ inclusion complex with pSC[4]A–ZnSQDs.

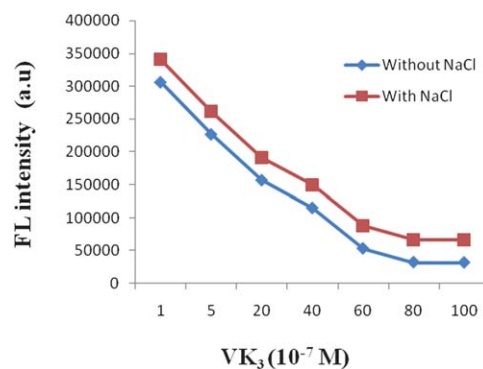


Fig. 6 Influence of NaCl ionic strength on the fluorescence quenching intensity of pSC[4]A–ZnSQDs system.

According to the literature,¹² a good size/shape fitting is necessary between the host and guest for the formation of a strong host–guest inclusion complex. Naphthalene (aromatic part of VK₃) is 0.5 nm wide²⁰ which exactly matches with the hydrophobic cavity of pSC[4]A.¹² In contrast to the cavity size of pSC[4]A, the big molecular size of other vitamins (VK₁ – 2.22 nm; VA – 1.30 nm; VB₂ – 1.13 nm; VC – 0.70 nm; VD₃ – 1.54 nm; VE – 1.78 nm) restricts the formation of the inclusion complex. Hence, pSC[4]A can selectively include VK₃ into its cavity by hydrophobic interaction on the surface of QDs, which obstructs the radiative path of QDs and hence quenches the FL intensity.^{7,16}

The quenching behaviour of VK₃ was inspected by the Stern–Volmer kinetics model.²¹ The Stern–Volmer plot is obtained from FL intensity measurements consequently with the addition of VK₃ in pSC[4]A–ZnSQDs. The Stern–Volmer plot reveals that the plot is linear up to the concentration of 1×10^{-6} M of VK₃ and then starts curving upwards (Fig. S5, ESI†). This clearly indicates that the quenching process occurs by a static mechanism till the concentration of 1×10^{-6} M of VK₃ and at higher concentrations quenching occurs *via* a dynamic mechanism. The unique UV-visible absorption spectra (Fig. S6, ESI†) and hypsochromic shift in FL spectra with the addition of VK₃ in pSC[4]A–ZnSQDs also supported the static quenching mechanism process.²²

Furthermore, below 1×10^{-6} M, the obtained experimental data of the Stern–Volmer plot can be satisfactorily fitted by a linear regression calibration equation (Fig. 7). A good linear relationship

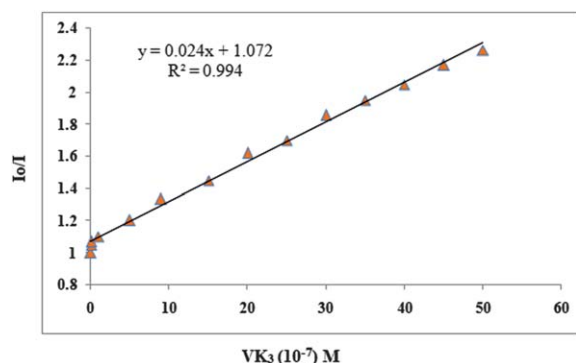


Fig. 7 The Stern–Volmer plot in the linear range (between 5×10^{-9} and 1×10^{-6} M); data plotted as I_0/I vs. $[VK_3]$.

($r > 0.99$) could be used to determine VK_3 . The limit of detection calculated by 3σ IUPAC criteria was 80 nM. Thus, the proposed sensor is better than the previously reported VK_3 sensors²³ (Table S1, ESI†).

Application of this probe in real samples was investigated by the analysis of a VK_3 containing commercial preparation. The solution preparation of pharmaceutical samples is described in ESI†. The standard addition method was applied to evaluate the validity of the proposed sensor. There was no interference observed by the accompanying compound, indicating the specificity of the probe. The result obtained with an excellent recovery (between 98% and 103.7%) in each product (Table S2, ESI†) confirms that the proposed sensor can effectively be used to determine the real content of VK_3 in pharmaceutical products.

In conclusion, here we developed a highly sensitive and selective optical nanoprobe for menadione (VK_3) determination. To the best of our knowledge, this is the first use of calix–QDs assembly for the detection of vitamins. This sensor is based on FL quenching by VK_3 through host–guest interaction with calixarene coated ZnSQDs. The detection limit for VK_3 recognition by the ultrasensitive probe is 80 nM in pharmaceutical commercial samples with almost 100% recovery. The simple, selective and sensitive approach of this method holds promise for application in future trends in biology.

Acknowledgements

Financial assistance from UGC, New Delhi is gratefully acknowledged.

Notes and references

- S. Zhu and Y. Ma, *Chin. J. Anal. Chem.*, 1998, **26**, 184.
- (a) M. Ishibashi, M. Arai, S. Tanaka, K. Onda and T. Hirano, *Biol. Pharm. Bull.*, 2012, **35**, 10; (b) R. Perez-Soler, Y. Zou, T. Li, C. Tornos and Y. Ling, *J. Clin. Oncol.*, 2006, **24**, (Abstr 3036); (c) J. M. Jamison, J. Gilloteaux, H. S. Taper and J. L. Summers, American Society for Nutritional Sciences, *J. Nutr.*, 2001, **131**, 158S; (d) R. T. Chlebowski, J. B. Block, M. F. Dietrich, E. Octay, N. Barth, R. Yanagihara, C. Gota and I. Ali, *Proc. Am. Assoc. Canc. Res.*, 1983, **24**, 165.
- (a) Y. Ruan, F. Duan, Y. Ying and X. Fan, *Fenxi Huaxue*, 1988, **16**, 746; (b) H. Kofler, *Helv. Chim. Acta*, 1945, **28**, 702; (c) Y. Haroom, D. S. Bacon and A. J. Sadowski, *Biomed. Chromatogr.*, 1987, **2**, 4; (d) L. Z. Wang, C. S. Ma, X. L. Zhang and L. Xu, *Microchem. J.*, 1994, **50**, 101.
- (a) Y. F. Chen and Z. Rosenzweig, *Anal. Chem.*, 2002, **74**, 5132; (b) C. Han and H. Li, *Chin. Chem. Lett.*, 2008, **19**, 215.
- (a) S. Zhang, A. Palkar and L. Echegoyen, *Langmuir*, 2006, **22**, 10732; (b) S. Zhang and L. Echegoyen, *Org. Lett.*, 2004, **6**, 791.
- (a) G. Patel and S. Menon, *Chem. Commun.*, 2009, 3563; (b) A. Pandya, K. V. Joshi, N. R. Modi and S. K. Menon, *Sens. Actuators, B*, 2012, **168**, 54; (c) G. Patel, A. Kumar, U. Pal and S. K. Menon, *Chem. Commun.*, 2009, 1849.
- (a) H. Li, Y. Zhang, X. Wang, D. Xiong and Y. Bai, *Mater. Lett.*, 2007, **61**, 1474; (b) T. Jin, F. Fujii, H. Sakata, M. Tamura and M. Kinjo, *Chem. Commun.*, 2005, 4300; (c) X. Wang, J. Wu, F. Li and H. Li, *Nanotechnology*, 2008, **19**, 20550.
- (a) C. J. Murphy, *Anal. Chem.*, 2002, **74**, 520A; (b) A. P. Alivisatos, *Nat. Biotechnol.*, 2004, **22**, 47.
- L. Shen, X. Cui, H. Qi and C. Zhang, *J. Phys. Chem. C*, 2007, **111**, 8172.
- (a) S. K. Mehta, Khushboo and A. Umarb, *Talanta*, 2011, **85**, 2411; (b) F. Zhang, C. Li, X. Li, X. Wang, Q. Wan, Y. Xian, L. Jin and K. Yamamoto, *Talanta*, 2006, **68**, 1353; (c) A. Mandal, A. Dandapat and G. De, *Analyst*, 2012, **137**, 765.
- A. G. Ghosh, M. K. Naskar, A. Patra and M. Chatterjee, *Opt. Mater.*, 2006, **28**, 1047.
- (a) H. Li and F. Qu, *Chem. Mater.*, 2007, **19**, 4141; (b) H. Li and F. Qu, *J. Mater. Chem.*, 2007, **17**, 3536.
- US Pat., 5952526, 1999.
- (a) A. F. D. Mamor, R. M. Cleverley and M. L. Zapata-Ormachea, *Chem. Rev.*, 1998, **98**, 2495; (b) C. D. Gutsche, *Calixarenes, an Introduction*, Royal Society of Chemistry, Cambridge, UK, 2008, p. 25.
- F. Qua, X. Zhoua, J. Xua, H. Lia and G. Xieb, *Talanta*, 2009, **78**, 1359.
- (a) Q. Wang, Y. C. Kuo, Y. W. Wang, G. Shin, C. Ruengruglikit and Q. R. Huang, *J. Phys. Chem. B*, 2006, **110**, 16860; (b) S. Jeong, M. Achermann, J. Nanda, S. Ivanov, V. I. Klimov and J. A. Hollingsworth, *J. Am. Chem. Soc.*, 2005, **127**, 10126.
- (a) Q. Lu, J. Gu, H. Yu, C. Liu, L. Wang and Y. Zhou, *Spectrochim. Acta, Part A*, 2007, **68**, 15; (b) Y. Zhou, H. Xu, L. Wu, C. Liu, Q. Lu and L. Wang, *Spectrochim. Acta, Part A*, 2008, **71**, 597.
- (a) N. R. Modi, B. R. Mistry, K. V. Joshi and S. K. Menon, *J. Inclusion Phenom. Macrocyclic Chem.*, 2011, **70**, 121; (b) B. R. Mistry, K. V. Joshi, N. R. Modi, D. Shashtri and S. K. Menon, *J. Inclusion Phenom. Macrocyclic Chem.*, 2011, **73**, 295.
- W. Yang and M. M. de Villiers, *AAPS J.*, 2005, **7**, E241.
- X. Wang and M. L. Brusseau, *Environ. Sci. Technol.*, 1995, **29**, 2346.
- J. R. Lakowicz, *Principles of Fluorescence Spectroscopy*, Kluwer Academic/Plenum Publishers, New York, 1999, ch. 8, pp. 238–264.
- C. C. Carrion, B. Lendl, B. M. Simonet and M. Valcarcel, *Anal. Chem.*, 2011, **83**, 8093.
- (a) J. J. Berzas Nevado, J. A. Murillo Pulgarín and M. A. Gómez Laguna, *Talanta*, 2000, **53**, 951; (b) Z. Chang-zhi, L. Ying, D. U. Hong, X. U. Hua-jun and J. Kui, *Chem. Res. Chin. Univ.*, 2010, **26**, 742; (c) U. Tas, K. Yilmaz and G. Somer, *Türk. J. Chem.*, 2011, **35**, 201; (d) Nashwa and M. H. Rizk, *Mikrochim. Acta*, 2002, **138**, 53; (e) Y. Huang, Z. Chen and Z. Zhang, *Anal. Sci.*, 1999, **15**, 1227.